Editors' Suggestion

Geodesic Path for the Minimal Energy Cost in Shortcuts to Isothermality

Geng Li,[1] Jin-Fu Chen,[2,1] C. P. Sun,[1,2] and Hui Dong[1,*]

[1]*Graduate School of China Academy of Engineering Physics, Beijing 100193, China*

[2]*Beijing Computational Science Research Center, Beijing 100193, China*

(Received 26 October 2021; revised 23 February 2022; accepted 3 May 2022; published 10 June 2022)

Shortcuts to isothermality are driving strategies to steer the system to its equilibrium states within finite time, and enable evaluating the impact of a control promptly. Finding the optimal scheme to minimize the energy cost is of critical importance in applications of this strategy in pharmaceutical drug tests, biological selection, and quantum computation. We prove the equivalence between designing the optimal scheme and finding the geodesic path in the space of control parameters. Such equivalence allows a systematic and universal approach to find the optimal control to reduce the energy cost. We demonstrate the current method with examples of a Brownian particle trapped in controllable harmonic potentials.

DOI: 10.1103/PhysRevLett.128.230603

Introduction.—Boosting a system to its steady state is critical to promptly evaluating the impact of a control [1–10]. In biological systems, the quest to timely evaluate the impact of therapy or genotypes posts a requirement to steer the system to reach its steady state with a considerable tunable rate [1–5]. In adiabatic quantum computation, the task of solving the optimization problem is converted to the problem of driving systems from a trivial ground state to another nontrivial ground state. The speedup of the computational process needs to steer the system to the target ground state in finite time [6–8]. These quests to tune the system within finite time while keep it in equilibrium are eagerly needed.

Shortcuts to isothermality were proposed as finite-time driving strategies to steer the system evolving along the path of instantaneous equilibrium states [11]. The strategy has been applied in reducing transition time between equilibrium states [12–14], improving the efficiency of free-energy estimation [15], constructing finite-time heat engines [16–18], and controlling biological evolutions [4,5]. The cost of the finite-time operation is the additional energy cost due to irreversibility posted by the fundamental thermodynamic law. Minimizing such a cost is in turn relevant to optimize the heat engine [19–21] and reconstruct the energy landscape of biological macromolecules [22–24]. A question arises naturally, how to find the optimal control protocol to minimize the irreversible energy cost in shortcuts to isothermality.

In this Letter, we present a systematic approach for finding the optimal protocol to minimize the energy cost. In Fig. 1, we show the equivalence of designing the optimal control to finding the geodesic path on a Riemannian manifold, spanned by the control parameters [25–29]. In turn, the powerful tools developed in geometry are adapted for solving the optimal control protocol. Our scheme is exemplified with a single Brownian particle in the harmonic potential with controllable stiffness and central position.

Geometric approach.—The system is described by the Hamiltonian $H_o(\vec{x},\vec{p},\vec{\lambda}) = \sum_i p_i^2/2 + U_o(\vec{x},\vec{p},\vec{\lambda})$ with the coordinate $\vec{x} \equiv (x_1, x_2, \ldots, x_N)$ and the momentum $\vec{p} \equiv (p_1, p_2, \ldots, p_N)$. It is immersed in a thermal reservoir with a constant temperature T. $\vec{\lambda}(t) \equiv (\lambda_1, \lambda_2, \ldots, \lambda_M)$ are time-dependent control parameters. For simplicity, we have set the mass of the system as a unit. In the shortcut scheme, an auxiliary Hamiltonian $H_a(\vec{x},\vec{p},t)$ is added to steer the system evolving along the instantaneous equilibrium states of the original Hamiltonian H_o in the finite-time interval τ

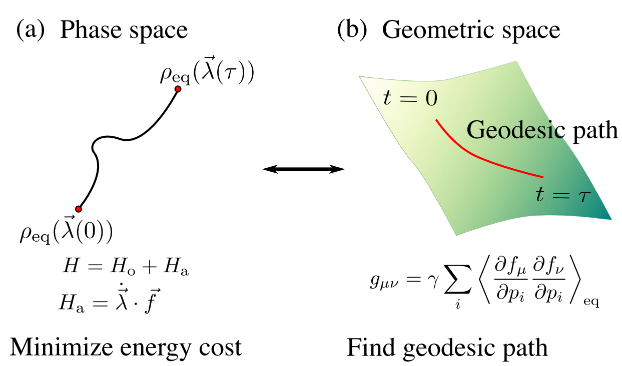

FIG. 1. The equivalence between designing the optimal control protocol and finding the geodesic path in the parametric space. (a) The evolution of the system controlled by the shortcut scheme. An auxiliary Hamiltonian $H_a = \dot{\vec{\lambda}} \cdot \vec{f}$ is added to steer the evolution along the instantaneous equilibrium state $\rho_{\rm eq}(\vec{\lambda}(t))$ of the original Hamiltonian H_o. Designing the optimal control protocol normally requires minimizing the energy cost in the shortcut scheme. (b) The geodesic path in the equivalent geometric space. We can convert the designing task into finding the geodesic path in the geometric space with the metric $g_{\mu\nu} = \gamma \sum_i \langle \partial_{p_i} f_\mu \partial_{p_i} f_\nu \rangle_{\rm eq}$.

with boundary conditions $H_a(0)=H_a(\tau)=0$. The dynamical evolution under the total Hamiltonian $H = H_o + H_a$ is described by the Langevin equation as

$$\dot{x}_i = \frac{\partial H}{\partial p_i},$$
$$\dot{p}_i = -\frac{\partial H}{\partial x_i} - \gamma \dot{x}_i + \xi_i(t), \tag{1}$$

where γ is the dissipation rate and $\vec{\xi} \equiv (\xi_1, \xi_2, \ldots, \xi_N)$ are random variables of the Gaussian white noise. The evolution equation of the system distribution $\rho(\vec{x}, \vec{p}, t) = \delta(\vec{x} - \vec{x}(t))\delta(\vec{p} - \vec{p}(t))$ for a trajectory $(\vec{x}(t), \vec{p}(t))$ is described by the Liouville equation as $\partial_t \rho = -\sum_i [\partial_{x_i}(\dot{x}_i \rho) + \partial_{p_i}(\dot{p}_i \rho)]$. By averaging over different noise realizations $\vec{\xi}(t)$ and a given initial distribution $P(\vec{x}(0), \vec{p}(0))$, we obtain the evolution of the observable probability distribution $P(\vec{x},\vec{p},t) \equiv \langle \rho(\vec{x},\vec{p},t) \rangle_{\vec{\xi}} = \iint D[\vec{x}(t)] D[\vec{p}(t)] \mathscr{T}[\vec{x}(t), \vec{p}(t)] \delta(\vec{x} - \vec{x}(t)) \delta(\vec{p} - \vec{p}(t))$ as [30]

$$\frac{\partial P}{\partial t} = \sum_i \left[-\frac{\partial}{\partial x_i}\left(\frac{\partial H}{\partial p_i} P\right) + \frac{\partial}{\partial p_i}\left(\frac{\partial H}{\partial x_i} P + \gamma \frac{\partial H}{\partial p_i} P\right) + \frac{\gamma \partial^2 P}{\beta \partial p_i^2}\right], \tag{2}$$

where $\beta \equiv 1/(k_B T)$ is the inverse temperature with the Boltzmann constant k_B. Here, $\mathscr{T}[\vec{x}(t), \vec{p}(t)]$ is the probability of the trajectory $(\vec{x}(t), \vec{p}(t))$ associated with a noise realization $\vec{\xi}(t)$ and the given initial distribution $P(\vec{x}(0), \vec{p}(0))$ [31,32]. The exact definition is presented in Supplemental Material [30]. To ensure the instantaneous equilibrium distribution

$$P(\vec{x}, \vec{p}, t) = P_{\mathrm{eq}}(\vec{x}, \vec{p}, \vec{\lambda}) = \mathrm{e}^{\beta[F(\vec{\lambda}) - H_o(\vec{x}, \vec{p}, \vec{\lambda})]}, \tag{3}$$

the auxiliary Hamiltonian is proved [11] to have the form $H_a(\vec{x}, \vec{p}, t) = \dot{\vec{\lambda}} \cdot \vec{f}(\vec{x}, \vec{p}, \vec{\lambda})$ with $\vec{f}(\vec{x}, \vec{p}, \vec{\lambda})$ satisfying

$$\sum_i \left[\frac{\gamma}{\beta} \frac{\partial^2 f_\mu}{\partial p_i^2} - \gamma p_i \frac{\partial f_\mu}{\partial p_i} + \frac{\partial f_\mu}{\partial p_i} \frac{\partial U_o}{\partial x_i} - p_i \frac{\partial f_\mu}{\partial x_i}\right] = \frac{dF}{d\lambda_\mu} - \frac{\partial U_o}{\partial \lambda_\mu}, \tag{4}$$

where $F \equiv -\beta^{-1} \ln[\iint d\vec{x} d\vec{p} \exp(-\beta H_o)]$ is the free energy. The boundary conditions are presented explicitly as $\dot{\vec{\lambda}}(0) = \dot{\vec{\lambda}}(\tau) = 0$.

The cost of the energy in the shortcut scheme is evaluated by the average work $W \equiv \langle \int_0^\tau dt \partial_t H \rangle_{\vec{\xi}}$ [33–36], explicitly as

$$W = \Delta F + \gamma \sum_i \int_0^\tau dt \iint d\vec{x} d\vec{p} \left(\frac{\partial H_a}{\partial p_i}\right)^2 P_{\mathrm{eq}}, \tag{5}$$

where $\Delta F = F(\vec{\lambda}(\tau)) - F(\vec{\lambda}(0))$ is the free energy difference. We remark that there is only a partial derivative to momentum in Eq. (5) due to the vanishing probability $P_{\mathrm{eq}}(\vec{x}, \vec{p}, \vec{\lambda})$ for the large momentum $\vec{p}$. A detailed derivation of Eq. (5) is presented in Supplemental Material [30]. To consider the finite-time effect, we define the irreversible work $W_{\mathrm{irr}} \equiv W - \Delta F$, which follows

$$W_{\mathrm{irr}} = \gamma \sum_{\mu\nu i} \int_0^\tau dt \dot{\lambda}_\mu \dot{\lambda}_\nu \left\langle \frac{\partial f_\mu}{\partial p_i} \frac{\partial f_\nu}{\partial p_i} \right\rangle_{\mathrm{eq}}, \tag{6}$$

with $\langle \cdot \rangle_{\mathrm{eq}} = \iint d\vec{x} d\vec{p} [\cdot] P_{\mathrm{eq}}$. It follows from Eq. (6) that the integrand scales as τ^{-2} through reducing the time $s \equiv t/\tau$, which results in the $1/\tau$ scaling [25] of the irreversible work, i.e., $W_{\mathrm{irr}} \propto 1/\tau$. Such a $1/\tau$ scaling, predicted in various finite-time studies [20,37–46], was recently verified for the ideal gas system [47] at the long-time limit. It is worth noting that in the shortcut scheme the current scaling is valid for any duration time τ with no requirement of the long-time limit [25,27,43,48,49].

In the space of thermodynamic equilibrium states marked by the control parameters $\vec{\lambda}$, we define a positive semidefinite metric

$$g_{\mu\nu} = \gamma \sum_i \left\langle \frac{\partial f_\mu}{\partial p_i} \frac{\partial f_\nu}{\partial p_i} \right\rangle_{\mathrm{eq}}, \tag{7}$$

whose positive semidefiniteness is proved in Supplemental Material [30]. This metric induces a Riemannian manifold on the space of thermodynamic equilibrium states, in which the distance of a shortest curve connecting two equilibrium states is characterized via the thermodynamic length [25,27–29,48] as $\mathcal{L} = \int_0^\tau dt \sum_{\mu\nu} \sqrt{\dot{\lambda}_\mu \dot{\lambda}_\nu g_{\mu\nu}}$. It provides a lower bound of the irreversible work W_{irr} as

$$W_{\mathrm{irr}} \geq \frac{\mathcal{L}^2}{\tau}, \tag{8}$$

which is obtained by using the Cauchy-Schwarz inequality [27]. The lower bound is reached with the optimal control scheme $\vec{\lambda}(t)$ $(0 < t < \tau)$, determined by the geodesic equation

$$\ddot{\lambda}_\mu + \sum_{\nu\kappa} \Gamma^\mu_{\nu\kappa} \dot{\lambda}_\nu \dot{\lambda}_\kappa = 0, \tag{9}$$

with the given boundary conditions $\vec{\lambda}(0)$ and $\vec{\lambda}(\tau)$. Here, the Christoffel symbol is defined as $\Gamma^\mu_{\nu\kappa} \equiv \frac{1}{2} \sum_\iota (g^{-1})_{\iota\mu} (\partial_{\lambda_\kappa} g_{\iota\nu} + \partial_{\lambda_\nu} g_{\iota\kappa} - \partial_{\lambda_\iota} g_{\nu\kappa})$. For the case with the single control parameter $\lambda(t)$, the analytical solution [28] for Eq. (9) is obtained as $\dot{\lambda}(t) = [\lambda(\tau) - \lambda(0)] g(\lambda(t))^{-1} / \int_0^\tau dt' g(\lambda(t'))^{-1}$, with $g = \gamma \langle (\partial_p f)^2 \rangle_{\mathrm{eq}}$. For the case with multiple parameters, the shooting method is an available option which treats the two-point boundary-value problem as an initial-value problem [50]. See Supplemental Material for details about the shooting method to our problems [30].

The strategy of current formalism is shown in Fig. 1. First, we obtain the control operators $\vec{f}(\vec{x},\vec{p},\vec{\lambda})$ in Fig. 1(a) by solving Eq. (4). Second, the metric $g_{\mu\nu}$ in Fig. 1(b) for the parametric space is calculated via Eq. (7). Finally, the optimal control is obtained by solving the geodesic equation in Eq. (9). The current strategy provides an effective approach to find the optimal control to minimize the energy cost, i.e., the total work done during the shortcut-to-isothermal process. The strategy is illustrated through two examples with one or two control parameters as follows.

Brownian motion in the harmonic potential.—The Brownian particle is trapped by the one-dimensional breathing harmonic potential with tunable stiffness $\lambda(t)$ under the Hamiltonian $H_o(x,p,\lambda)=p^2/2+\lambda(t)x^2/2$. Its auxiliary Hamiltonian was derived in Ref. [11] as $H_a(x,p,t)=\dot{\lambda}f(x,p,\lambda)$ with $f=1/(4\gamma\lambda)[(p-\gamma x)^2+\lambda x^2]$. The metric in Eq. (7) in this case reduces to [30]

$$g=\frac{\lambda+\gamma^2}{4\gamma\beta\lambda^3}. \tag{10}$$

And the lower bound of the irreversible work is reached by the protocol satisfying the geodesic equation $\ddot{\lambda}+\dot{\lambda}^2\partial_\lambda g/(2g)=0$. The solution

$$\lambda_{\rm GP}(t)=\frac{\sqrt{1+2\gamma^2(m_s-n_st/\tau)}+1}{2(m_s-n_st/\tau)}, \tag{11}$$

offers an optimal protocol to minimize the energy cost in the shortcut scheme. Here, $m_s=1/\lambda(0)+\gamma^2/[2\lambda(0)]$ and $n_s=1/\lambda(0)+\gamma^2/[2\lambda(0)]-1/\lambda(\tau)-\gamma^2/[2\lambda(\tau)]$ are constants for single control-parameter case. And the irreversible work of the geodesic protocol (GP) reaches its minimum $W_{\rm irr}^{\rm min}=\int_0^\tau\dot{\lambda}^2gdt=n_s^2/\tau$, which is consistent with the lower bound given by the thermodynamic length $\mathcal{L}=\int_0^\tau\sqrt{\dot{\lambda}^2g}dt=n_s$ through the relation $W_{\rm irr}^{\rm min}=\mathcal{L}^2/\tau$.

Underdamped Brownian motion with two control parameters.—We consider a Brownian particle moving in the one-dimensional harmonic potential with Hamiltonian $H_o(x,p,\lambda)=p^2/2+\lambda_1x^2/2-\lambda_2x$. The auxiliary Hamiltonian for the shortcut scheme takes the form [30] $H_a(x,p,t)=\sum_{\mu=1}^2\dot{\lambda}_\mu f_\mu(x,p,\lambda_1,\lambda_2)$ with

$$f_1=\frac{(p-\gamma x)^2+\lambda_1x^2}{4\gamma\lambda_1}-\frac{\lambda_2p}{2\lambda_1^2}+\left(\frac{\gamma\lambda_2}{2\lambda_1^2}-\frac{\lambda_2}{2\gamma\lambda_1}\right)x,$$
$$f_2=\frac{p}{\lambda_1}-\frac{\gamma x}{\lambda_1}. \tag{12}$$

The metric in Eq. (7) for the control parameters $\vec{\lambda}$ is obtained as

$$g=\begin{pmatrix}\frac{1}{4\beta\gamma\lambda_1^2}+\frac{\gamma}{4\beta\lambda_1^3}+\frac{\gamma\lambda_2^2}{\lambda_1^4} & -\frac{\gamma\lambda_2}{\lambda_1^3}\\ -\frac{\gamma\lambda_2}{\lambda_1^3} & \frac{\gamma}{\lambda_1^2}\end{pmatrix}. \tag{13}$$

The geodesic equation follows

$$\ddot{\lambda}_1-\frac{\dot{\lambda}_1^2(3\gamma^2+2\lambda_1)}{2\lambda_1(\gamma^2+\lambda_1)}=0,$$
$$\ddot{\lambda}_2-\frac{2\dot{\lambda}_1\dot{\lambda}_2}{\lambda_1}+\frac{\dot{\lambda}_1^2\lambda_2(\gamma^2+2\lambda_1)}{2\lambda_1^2(\gamma^2+\lambda_1)}=0, \tag{14}$$

with the boundary conditions $\vec{\lambda}(0)$ and $\vec{\lambda}(\tau)$.

The optimal scheme can be obtained by solving equations above using a general numerical method, i.e., the shooting method [50]. Here, we first solve these equations numerically to provide a general perspective on our scheme. With the initial point $\vec{\lambda}(0)$, we choose an initial rate $\dot{\vec{\lambda}}(0+)$ and solve the geodesic equation with the Euler algorithm to obtain a trial solution $\vec{\lambda}^{\rm tri}(\tau)$. Newton's method is utilized for updating the rate $\dot{\vec{\lambda}}(0+)$ to reduce the distance between the trial solution $\vec{\lambda}^{\rm tri}(\tau)$ and the target point $\vec{\lambda}(\tau)$. In the simulation, we have chosen the parameters $\vec{\lambda}(0)=(1,1)$, $\vec{\lambda}(\tau)=(16,2)$, $k_BT=1$, and $\gamma=1$. The geodesic path for the optimal control is illustrated as $\vec{\lambda}^{{\rm GP},n}(t)$ (triangles) in Fig. 2.

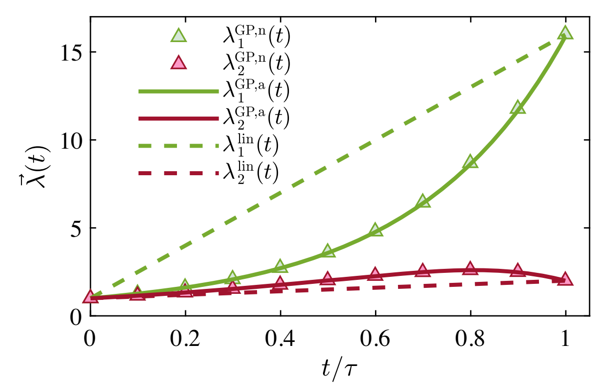

FIG. 2. Geodesic protocols for the control with two parameters. In the simulation, we have set the temperature and the dissipation rate as $k_BT=1$ and $\gamma=1$. The parameters change from the initial point $\vec{\lambda}(0)=(1,1)$ to the final point $\vec{\lambda}(\tau)=(16,2)$. The triangles represent the numerical geodesic protocol $\vec{\lambda}^{{\rm GP},n}(t)$ while the solid lines represent the analytical geodesic protocol $\vec{\lambda}^{{\rm GP},a}(t)$. The dashed lines represent the linear protocol $\vec{\lambda}^{\rm lin}(t)$. The numerical geodesic protocol (triangles) coincides well with the analytical geodesic protocol (solid lines).

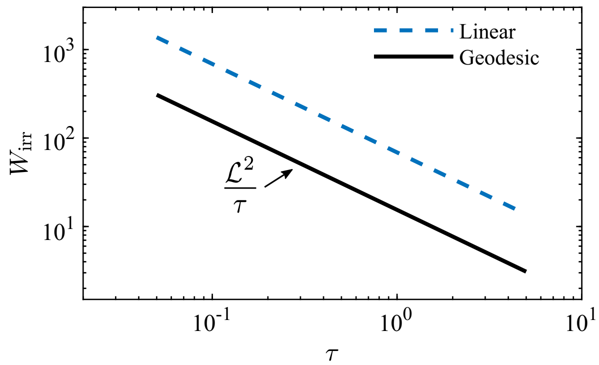

FIG. 3. The irreversible work of the geodesic protocol (black solid line) and the linear protocol (blue dashed line). The black solid line represents the lower bound given by the thermodynamic length, i.e., Eq. (8). The irreversible cost given by the geodesic protocol is lower than that from the linear protocol.

Fortunately, the analytical geodesic protocol for Eq. (14) can be obtained as

$$\dot{\lambda}_1 = \frac{w_b}{\tau}\sqrt{\frac{\lambda_1^3}{\lambda_1+\gamma^2}},$$
$$\frac{\lambda_2}{\lambda_1} = m_b t/\tau + n_b, \tag{15}$$

where $w_b = -[2\sqrt{1+\gamma^2/\lambda_1} + \ln(\sqrt{1+\gamma^2/\lambda_1}-1) - \ln(\sqrt{1+\gamma^2/\lambda_1}+1)]|_{\lambda_1(0)}^{\lambda_1(\tau)}$, $m_b = [\lambda_2(\tau)\lambda_1(0) - \lambda_2(0)\lambda_1(\tau)]/[\lambda_1(\tau)\lambda_1(0)]$, and $n_b = \lambda_2(0)/\lambda_1(0)$ are constants. In Fig. 2, we show the match between the optimal control obtained from the numerical calculation $\vec{\lambda}^{\mathrm{GP},n}(t)$ (triangles) and the analytical solution $\vec{\lambda}^{\mathrm{GP},a}(t)$ (solid lines). For the comparison, we also show the protocol of the simple linear control $\vec{\lambda}^{\mathrm{lin}}(t) = [\vec{\lambda}(\tau) - \vec{\lambda}(0)]t/\tau + \vec{\lambda}(0)$.

To validate our results of optimization, we plot the irreversible work W_{irr} as a function of duration τ for both the geodesic path and the simple linear control in Fig. 3. The geodesic protocol results in a lower irreversible work than that from the simple linear protocol $\vec{\lambda}^{\mathrm{lin}}(t)$. The black solid line shows the analytical results $W_{\mathrm{irr}}^{\min} = \mathcal{L}^2/\tau$, where the thermodynamic length $\mathcal{L}$ is calculated as $\mathcal{L} = \int_0^\tau dt \sum_{\mu\nu}\sqrt{\dot{\lambda}_\mu\dot{\lambda}_\nu g_{\mu\nu}} = \sqrt{w_b^2/(4\beta\gamma) + \gamma m_b^2}$ and the blue dashed line represents the irreversible work of the linear protocol [30]. Figure 3 shows that the geodesic protocol can largely reduce the irreversible work, which therefore proves our findings about the geometric property of the control-parameter space in the shortcut scheme. Our findings simplify the procedure of finding the optimal control protocol in the shortcut scheme by applying the tools of Riemannian geometry.

Conclusions.—In summary, we have provided a geometric approach to find the optimal control scheme to steer the evolution of the system along the path of instantaneous equilibrium states to reduce the energy cost. The proven equivalence between designing the optimal control and finding the geodesic path in the parametric space allows the application of the methods developed in Riemannian geometry to solve the optimization problem in thermodynamics. We have applied our approach into the Brownian particle system tuned by both one and two control parameters to find the optimal control for reducing energy cost. Analytical results have verified that the geodesic protocol can largely reduce the irreversible work in the shortcut scheme. Our strategy shall provide an effective tool to design the optimal finite-time control with the lowest energy cost.

Our results demonstrate that the optimal control with the minimal energy cost to transfer the system between equilibrium states is to steer the system evolving along the geodesic path. Once the initial and final equilibrium states are given, the geodesic path is determined by the geodesic equation (9) for the given system. The dynamics of the system is covered by the metric $g_{\mu\nu}$ in Eq. (7) without the need to treat the system on a case-by-case basis. An intuitive determination of the performance of the controls is allowed with the proportional relation in Eq. (8) between the minimal energy cost and the square of the length of the geodesic path.

This work is supported by the National Natural Science Foundation of China (NSFC) (Grants No. 12088101, No. 11875049, No. U1930402, No. U1930403, and No. 12047549) and the National Basic Research Program of China (Grant No. 2016YFA0301201).

*hdong@gscaep.ac.cn

[1] D. Nichol, P. Jeavons, A. G. Fletcher, R. A. Bonomo, P. K. Maini, J. L. Paul, R. A. Gatenby, A. R. Anderson, and J. G. Scott, PLoS Comput. Biol. **11**, e1004493 (2015).
[2] N. Ahmad and Z. Mukhtar, Genomics **109**, 494 (2017).
[3] C. B. Ogbunugafor, C. S. Wylie, I. Diakite, D. M. Weinreich, and D. L. Hartl, PLoS Comput. Biol. **12**, e1004710 (2016).
[4] S. Iram, E. Dolson, J. Chiel, J. Pelesko, N. Krishnan, Özenç Güngör, B. Kuznets-Speck, S. Deffner, E. Ilker, J. G. Scott, and M. Hinczewski, Nat. Phys. **17**, 135 (2021).
[5] E. Ilker, Özenç Güngör, B. Kuznets-Speck, J. Chiel, S. Deffner, and M. Hinczewski, Phys. Rev. X **12**, 021048 (2022).
[6] T. Albash and D. A. Lidar, Rev. Mod. Phys. **90**, 015002 (2018).
[7] K. Takahashi, J. Phys. Soc. Jpn. **88**, 061002 (2019).
[8] D. Guéry-Odelin, A. Ruschhaupt, A. Kiely, E. Torrontegui, S. Martínez-Garaot, and J. G. Muga, Rev. Mod. Phys. **91**, 045001 (2019).
[9] X. Chen, A. Ruschhaupt, S. Schmidt, A. del Campo, D. Guéry-Odelin, and J. G. Muga, Phys. Rev. Lett. **104**, 063002 (2010).
[10] K. Funo, N. Lambert, F. Nori, and C. Flindt, Phys. Rev. Lett. **124**, 150603 (2020).

[11] G. Li, H. T. Quan, and Z. C. Tu, Phys. Rev. E **96**, 012144 (2017).
[12] J. A. C. Albay, S. R. Wulaningrum, C. Kwon, P.-Y. Lai, and Y. Jun, Phys. Rev. Research **1**, 033122 (2019).
[13] J. A. C. Albay, P.-Y. Lai, and Y. Jun, Appl. Phys. Lett. **116**, 103706 (2020).
[14] J. A. C. Albay, C. Kwon, P.-Y. Lai, and Y. Jun, New J. Phys. **22**, 123049 (2020).
[15] G. Li and Z. C. Tu, Phys. Rev. E **103**, 032146 (2021).
[16] N. Pancotti, M. Scandi, M. T. Mitchison, and M. Perarnau-Llobet, Phys. Rev. X **10**, 031015 (2020).
[17] K. Nakamura, J. Matrasulov, and Y. Izumida, Phys. Rev. E **102**, 012129 (2020).
[18] C. A. Plata, D. Guéry-Odelin, E. Trizac, and A. Prados, J. Stat. Mech. (**2020**) 093207.
[19] T. Schmiedl and U. Seifert, Phys. Rev. Lett. **98**, 108301 (2007).
[20] T. Schmiedl and U. Seifert, Europhys. Lett. **81**, 20003 (2008).
[21] Z. C. Tu, Phys. Rev. E **89**, 052148 (2014).
[22] E. Atılgan and S. X. Sun, J. Chem. Phys. **121**, 10392 (2004).
[23] F. M. Ytreberg, R. H. Swendsen, and D. M. Zuckerman, J. Chem. Phys. **125**, 184114 (2006).
[24] S. Vaikuntanathan and C. Jarzynski, Phys. Rev. Lett. **100**, 190601 (2008).
[25] P. Salamon and R. S. Berry, Phys. Rev. Lett. **51**, 1127 (1983).
[26] M. A. Nielsen, M. R. Dowling, M. Gu, and A. C. Doherty, Science **311**, 1133 (2006).
[27] G. E. Crooks, Phys. Rev. Lett. **99**, 100602 (2007).
[28] D. A. Sivak and G. E. Crooks, Phys. Rev. Lett. **108**, 190602 (2012).
[29] J.-F. Chen, C. P. Sun, and H. Dong, Phys. Rev. E **104**, 034117 (2021).
[30] See Supplemental Material at http://link.aps.org/supplemental/10.1103/PhysRevLett.128.230603 for detailed derivations of main-text equations.
[31] L. E. Reichl, *A Modern Course in Statistical Physics* (Wiley, New York, 1998).
[32] A. Imparato and L. Peliti, Phys. Rev. E **74**, 026106 (2006).
[33] C. Jarzynski, Phys. Rev. Lett. **78**, 2690 (1997).
[34] K. Sekimoto, *Stochastic Energetics* (Springer-Verlag GmbH, Berlin, 2010).
[35] U. Seifert, Rep. Prog. Phys. **75**, 126001 (2012).
[36] G. Li and Z. C. Tu, Phys. Rev. E **100**, 012127 (2019).
[37] F. L. Curzon and B. Ahlborn, Am. J. Phys. **43**, 22 (1975).
[38] C. Van den Broeck, Phys. Rev. Lett. **95**, 190602 (2005).
[39] M. Esposito, R. Kawai, K. Lindenberg, and C. Van den Broeck, Phys. Rev. Lett. **105**, 150603 (2010).
[40] Y. Wang and Z. C. Tu, Phys. Rev. E **85**, 011127 (2012).
[41] C. de Tomás, A. C. Hernández, and J. M. M. Roco, Phys. Rev. E **85**, 010104(R) (2012).
[42] A. Ryabov and V. Holubec, Phys. Rev. E **93**, 050101(R) (2016).
[43] V. Cavina, A. Mari, and V. Giovannetti, Phys. Rev. Lett. **119**, 050601 (2017).
[44] Y.-H. Ma, D. Xu, H. Dong, and C.-P. Sun, Phys. Rev. E **98**, 042112 (2018).
[45] Y.-H. Ma, D. Xu, H. Dong, and C.-P. Sun, Phys. Rev. E **98**, 022133 (2018).
[46] Z.-C. Tu, Front. Phys. **16**, 33202 (2021).
[47] Y.-H. Ma, R.-X. Zhai, J. Chen, C. P. Sun, and H. Dong, Phys. Rev. Lett. **125**, 210601 (2020).
[48] M. Scandi and M. Perarnau-Llobet, Quantum **3**, 197 (2019).
[49] J.-F. Chen, Y. Li, and H. Dong, Entropy **23**, 353 (2021).
[50] M. Berger, *A Panoramic View of Riemannian Geometry* (Springer, Berlin, Heidelberg, 2007).